Korean J. Chem. Eng., **27**(5), 1532-1537 (2010)
DOI: 10.1007/s11814-010-0245-0

$CaCO_3$ crystallization with feeding of aspartic acid

Jin-Ho Kim*, Sung Moon Song*, Jong Min Kim, Woo Sik Kim***, and In Ho Kim*,†**

*Department of Chemical Engineering, Chungnam National University, 220, Gung-dong, Yuseong-gu, Daejeon 305-764, Korea
**Department of Chemical Engineering, Dong A University, 840, Hadan-2dong, Saha-gu, Busan 204-714, Korea
***Department of Chemical Engineering, Kyunghee University, 1, Seocheon-dong, Yongin, Gyunggi-do 446-701, Korea
(*Received 9 September 2009 • accepted 6 January 2010*)

Abstract−Aspartic acid (Asp) was employed as the organic template in inducing the nucleation and growth of calcium carbonate. Crystallization experiments were carried out by the addition of Asp into the solution of sodium carbonate and calcium chloride. The effects of reaction time, dropping velocity of Asp and Na_2CO_3 solution were tested. The $CaCO_3$ crystals were analyzed by X-ray diffraction (XRD), field emission scanning electron microscope (FE-SEM) and Fourier transform infrared spectrometry (FT-IR). Two kinds of crystals were identified by FT-IR spectrum. In the presence of Asp, formation of vaterite is induced in crystallization solution. Also, under the initial condition of an excess amount of Asp, vaterite morphology is the major one. Various morphologies of $CaCO_3$ are made by changing dropping velocity of added Asp and Na_2CO_3.

Key words: Feeding, Calcium Carbonate, Aspartic Acid

INTRODUCTION

Calcium carbonate ($CaCO_3$) is one of the most plentiful mineral resources formed in natural environment. The precipitated calcium carbonate has increasingly attracted attention because of its use as an additive in paint, plastic, rubber, papers, adhesive and biomedical application. The application of calcium carbonate particles to industry is mainly determined by the polymorphs of $CaCO_3$. Calcium carbonate has three crystal polymorphs: rhombic calcite, needle-like aragonite and spherical vaterite. Calcite is usually the dominant polymorph at a high solution pH, low temperature and the most stable phase at room temperature under atmospheric conditions. While vaterite and aragonite are mostly produced at a low solution pH, high temperature, they transform to stable calcite. Synthetic conditions of calcite, aragonite and vaterite are different. Vaterite, which is the most unstable crystal morphology, is obtained by controlling the $CaCO_3$ solution composition. Calcite is abundant in nature and well utilized in industry due to regular crystal size and smooth surface.

Since Eq. (1) reaction is a gas-liquid one, its contact method affects the granularity and particle shape of $CaCO_3$ [1,2]. Also, this reaction has a high degree of flexibility and does not produce soluble byproduct. Eq. (2) is mainly used for large scale production. The gas-liquid reaction has little effect on $CaCO_3$ morphology because it makes water as byproduct. Since gas reactant flows over the liquid surface, Eq. (1) is difficult to realize in an industrial process.

$$Ca(OH)_2(aq)+CO_2(aq, gas)\rightarrow CaCO_3(solid)+H_2O(byproduct) \quad (1)$$

$$CaO(aq)+CO_2(gas)\rightarrow CaCO_3(solid) \quad (2)$$

$$CaCl_2(aq)+Na_2CO_3(aq)\rightarrow CaCO_3(sol)+2NaCl(byproduct) \quad (3)$$

†To whom correspondence should be addressed.
E-mail: ihkim@cnu.ac.kr

On the other hand, the liquid-liquid reaction for $CaCO_3$ crystallization makes both $CaCO_3$ crystals and NaCl byproduct as Eq. (3) [3-7]. Nucleation and growth of crystal are affected by NaCl because the byproduct has high ionic strength. However, this reaction is frequently used for $CaCO_3$ crystallization since the reaction easily controls saturation concentration in solution and produces various morphologies of $CaCO_3$ crystalline. It is also easy to make biominerals from $CaCO_3$ crystallization reaction by a liquid-liquid reaction with organic materials.

Previous reports showed that the polymorph of calcium carbonate is dependent on the operating conditions of crystallization, such as supersaturation [8], solution composition [9], pH [10], temperature [11], and presence of additives [12-19]. The effect of additives has been studied on the crystallization of calcium carbonate. Biomineralization produced biominerals with good mechanical property by adding amino acid to $CaCO_3$ [20,21]. For example, a shell of mollusca consists of 95% $CaCO_3$, which is made up of calcite and $CaCO_3$ layer structure. This layer structure's fracture toughness is thousands times as strong as that of simple $CaCO_3$ crystals. Manoli et al. discovered that the presence of lysine, glycine, alanine, polyglycine, polymethionine and polylysine in the supersaturated solutions stabilizes the vaterite polymorph [22]. They also reported that the presence of glutamic acid in the supersaturated solution stabilizes the vaterite polymorph [23]. According to Xie et al., various kinds of amino acid, such as L-cystine, L-tyrosine, DL-aspartic acid, L-lysine and the mixed systems of L-Tyr(or L-Lys)/Mg^{2+}, were used as effective modifiers to mediate the crystallization of $CaCO_3$. Amino acids used in this experiment influenced the morphology and crystal type of $CaCO_3$. Most tended to induce vaterite formation [24]. They found that, in chitosan gel, the formation of calcium carbontate is controlled by the kinetics to form hexagonal vaterite plates, and the high energy (001) planes are effectively stabilized by the stereochemically matched hydrogen bonding interactions of flexible chitosan chains [25]. Henderson et al. indicated that the pres-

ence of the carboxylic acids inhibited crystal growth and calcium carbonate solubility increased. No effect was observed with respect to enhanced calcium carbonate solubility as a function of carboxylic acid chain length [26]. In Tong's paper, the amino acid kinds on the interface of organic template and calcium carbonate have been searched to be rich in aspartic acid and glutamic acid. Thus, it can be assumed that the carboxyl groups of aspartic acid and glutamic acid provide abundant Ca^{2+} ions bonding sites [27]. Calcium carbonate crystals were precipitated in glycine-containing aqueous solutions using two methods: CO_3^{2-} dropping method or diffusion method. By modulating the dropping velocity and glycine concentration, they can control the morphologies and proportion of the acquired vaterite particles [28].

In the present work, we assume that morphologies of $CaCO_3$ crystals are affected by the dropping velocity of Asp and Na_2CO_3 solution into $CaCl_2$ solution. The analytical aims of the present study are to study the morphological change of $CaCO_3$ with field emission scanning electron microscope (FE-SEM), X-ray diffraction spectrometer (XRD) and Fourier transform infrared spectroscope (FT-IR), as well as to discuss the mechanism. FE-SEM was used to analyze morphology and crystal size. XRD was used to measure peak intensities and the presence of $CaCO_3$ polymorph. Two kinds of crystals were confirmed by FT-IR spectrum. Crystal morphology change with reaction time was identified with measured peak areas of XRD pattern and FT-IR data.

EXPERIMENTAL

1. Materials and Sample Preparation

All the chemicals, including calcium chloride ($CaCl_2$) (purity ≥99.0%), sodium carbonate (Na_2CO_3) (purity ≥99.0%) were of analytical grade and used without further purification. D, L-aspartic acids were purchased from Aldrich. Doubly deionized water was used to prepare aqueous solutions of $CaCl_2$ and Na_2CO_3 just before crystallization experiment.

2. Crystallization Reaction with Dropping Asp or Na_2CO_3 Solution

Experiments were performed in a thermostated double-wall Pyrex vessel at 25 °C, and the working volume was 1.0 L. Control crystallization solutions were prepared by mixing equal volumes (300 mL) of 0.1 M calcium chloride ($CaCl_2$), 0.1 M sodium carbonate (Na_2CO_3) and 0.1 M aspartic acid (Asp) solution. The calcium carbonate precipitation was started by injecting Na_2CO_3 and Asp solution into stirred 0.1 M $CaCl_2$ solution. The stirring speed was controlled around 300 rpm. The dropping velocity of Na_2CO_3 and Asp solution was in the range of 0-10 mL/min.

3. Characterization of Crystals

Samples of the product suspension were taken intermittently during reaction, and filtered immediately using a micromembrane filter with a 0.45 μm pore diameter. After being dried at 50 °C for 24 h, the solid residues were characterized by using SEM (JEOL JSM-

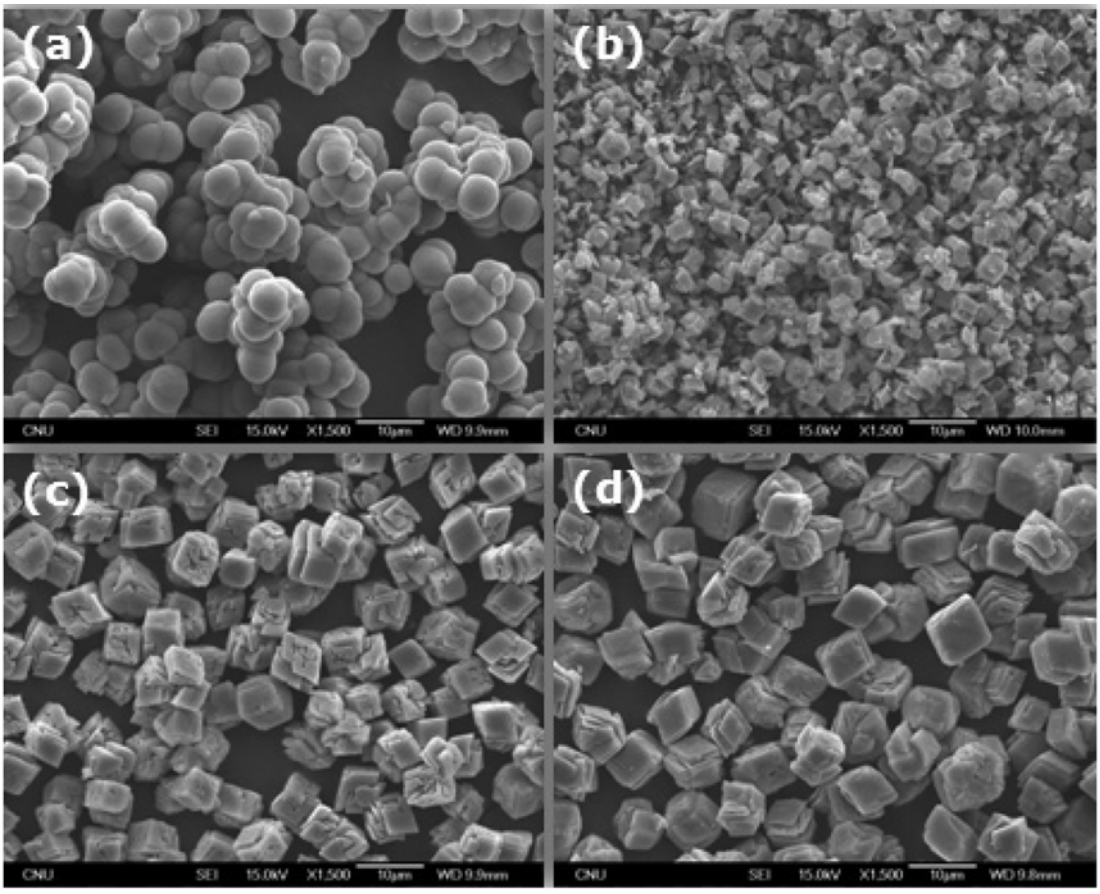

Fig. 1. SEM images of $CaCO_3$ by changing dropping velocity of Asp solution to $CaCl_2$ and Na_2CO_3 mixture; (a) dumping of Asp, (b) 1 mL/min, (c) 4 mL/min, (d) 10 mL/min.

7000F, Japan) for their crystal morphology and by multipurpose X-ray diffractometer (XRD) for calculating the ratio of calcite to vaterite of $CaCO_3$. XRD (Rigaku D/MAX-2200 Ultima/PC, Japan) measurements were conducted using Cu Kα radiation (40 keV, 30 mA) to identify the composition of the crystals. The scanning step was 0.02° and 2θ ranges from 10° to 80°. In addition, Fourier transform infrared spectroscopy (FT-IR) analysis was carried out by using KBr discs in the region of 4,000-600 cm^{-1} with a Shimadzu spectrophotometer (Rrestoge-21). From the data of the Joint Committee on Powder Diffraction Standards (JCPDS), it was compared with actual XRD data.

RESULTS AND DISCUSSION

The addition of Asp with different dropping velocities considerably influences $CaCO_3$ crystal morphology. Fig. 1(a) shows the shape of $CaCO_3$ crystals from the control experiment of 0.1 M $CaCl_2$ and Na_2CO_3 solution (pH=8.5, t=5 hr). In this case, we dumped all of Na_2CO_3 and Asp into $CaCl_2$ solution at the start. The other experiments were conducted under conditions of different Asp feeding speed. Only spherical vaterites are observed in Fig. 1(a). However, relatively small calcite crystals are observed under the Asp dropping velocity of 1 mL/min in Fig. 1(b). In case of 4 mL/min, the crystals in Fig. 1(c) are larger than that of Fig. 1(b). Crystal shape in Fig. 1(c) seems to be twisted rhombohedrally. Fig. 1(d) shows that the rhombohedral form of calcite crystals is more evident than in Fig. 1(c). Crystal of calcite in Fig. 1(d) is similar to the produced calcite in the paper [27], but different crystal shapes were obtained by them because experimental conditions were set up with various amounts of lysine (0-40 mg) into $CaCl_2$ solutions (0.5 M) and by

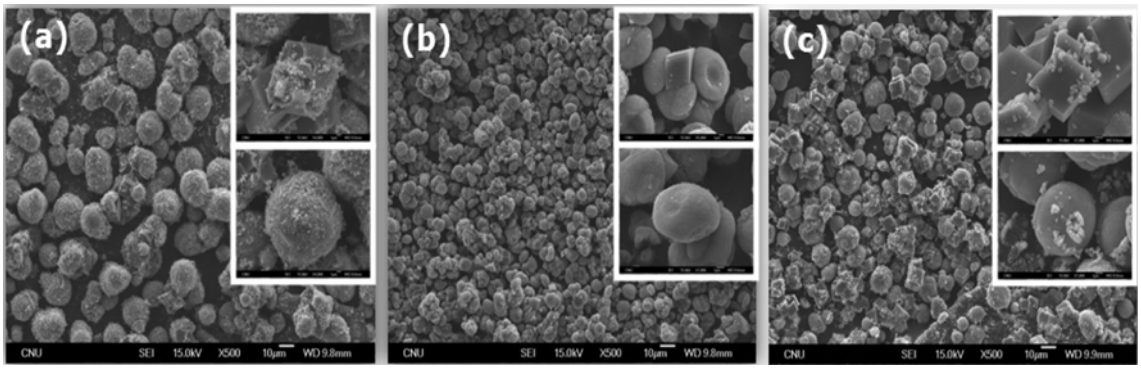

Fig. 2. SEM images of $CaCO_3$ by changing dropping velocity of Na_2CO_3 to $CaCl_2$ with a fixed dropping Asp solution at 2 mL/min; (a) 3.4 mL/min, (b) 6.0 mL/min, (c) 8.5 mL/min.

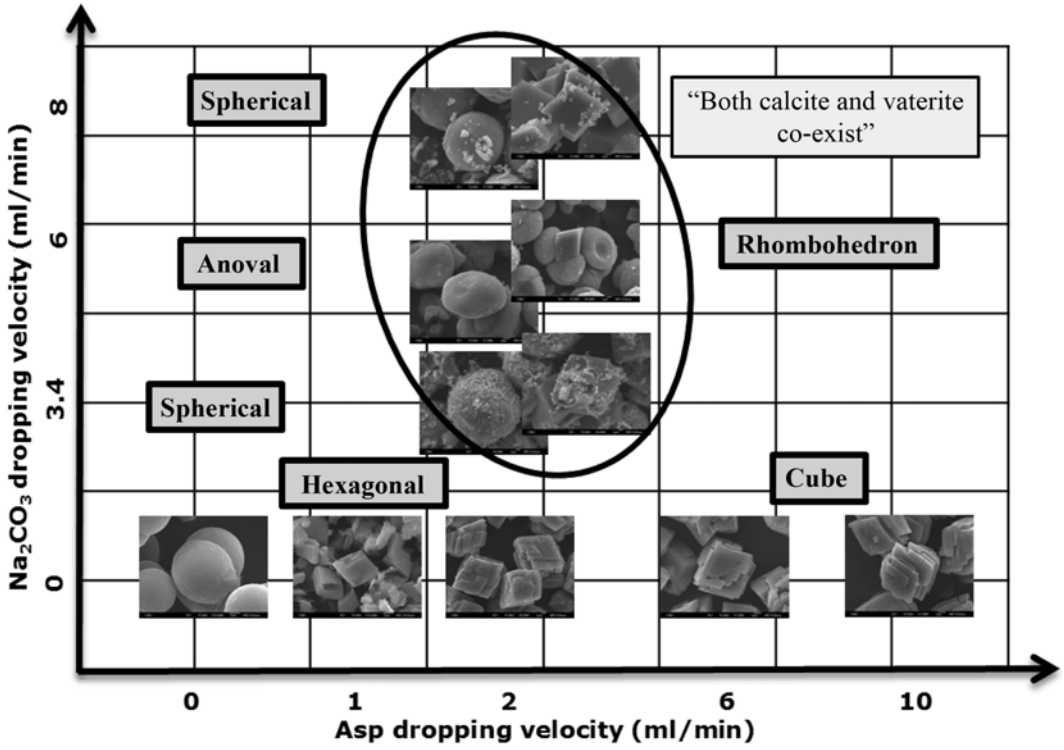

Fig. 3. Various morphologies of $CaCO_3$ crystals observed by SEM under different feed conditions of Na_2CO_3 and Asp into $CaCl_2$ solution.

plugging them slowly into Na_2CO_3 solutions (0.5 M) at 37 °C.

Rhombohedral calcite and spherical vaterite are appearing when we change Na_2CO_3 dropping velocity with a speed of Asp solution (2 mL/min). Fig. 2(a) shows imperfect $CaCO_3$ crystals under Na_2CO_3 dropping velocity of 3.4 mL/min. Phase of calcite and rough surface of vaterite crystals are observed. As shown in Fig. 2(b), definite rhombohedral calcite crystals appear, but vaterite crystals seem to be donut-like and an oval morphology. $CaCO_3$ polymorphs are found in Fig. 2(c). We can observe tiny powders on the surface of $CaCO_3$ crystals, and higher dropping velocity of Na_2CO_3 leads to small $CaCO_3$ crystals as an obvious form.

Two different methods were used to study the biomineralization of calcium carbonate with Asp. Changing dropping velocity of Asp and Na_2CO_3 has effects on the formation of crystals. Fig. 3 summarizes the morphology variation of all dropping solution experiments. The horizontal line represents the change of Asp dropping velocity and the vertical line stands for sodium carbonate dropping velocity. Spherical, hexagonal and cubic shapes are observed along the line of zero dropping velocity of sodium carbonate. With the increase of Asp dropping velocity, various calcite forms appear from spherical to cubic. Meanwhile, calcite and vaterite are appearing in a more complicated manner when sodium carbonate solution is fed with dropping of Asp solution.

Fig. 4 shows the time course of FT-IR spectra of calcium carbonate crystal, in which dropping was controlled at 6 mL/min of Na_2CO_3 solution and 2 mL/min of Asp. Among the characteristic IR peaks for calcite (711, 875, 1,087 and 1,478 cm^{-1}) and vaterite (744, 875 and 1,478 cm^{-1}), the peaks at 711 and 744 cm^{-1} were used to identify calcite and vaterite, respectively. We compared the intensity of calcite (711 cm^{-1}) with that of vaterite (744 cm^{-1}). Calcite and vaterite peaks appear in all the spectra, and the ratio of calcite to vaterite decreases until 5 h.

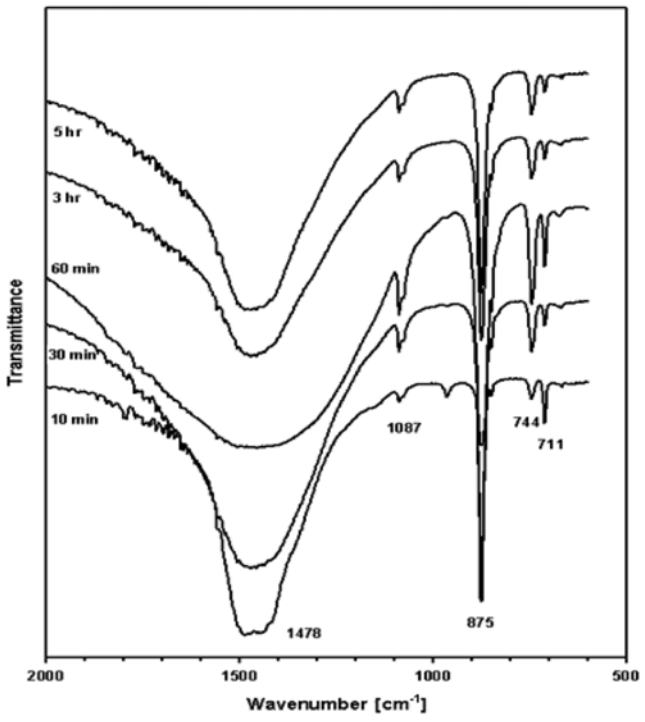

Fig. 4. Time course of FT-IR spectra of calcium carbonate crystal; 300 mL of 0.1 M Na_2CO_3 dropped at 6.0 mL/min with dropping Asp solution at 2 mL/min.

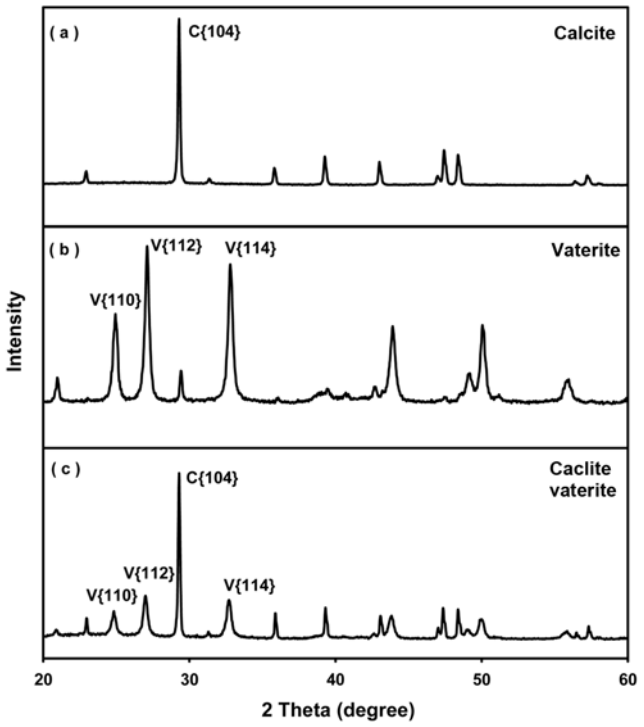

Fig. 5. The data of X-ray diffraction patterns of calcium carbonate after 5 hr of reaction; (a) dropping speed of Asp (1 mL/min), (b) dumping of Asp and (c) dropping speed of Asp (2 mL/min).

Specific peaks of calcite and vaterite crystals are displayed by XRD spectrometer. Fig. 5(a) XRD data is the result of crystallization reaction when Asp solution was dropped with a velocity of 1 mL/min. Only a specific calcite peak is observed in this data. Phase {104} of calcite most sharply appears in XRD patterns and the other calcite peaks are shown. All the reflections could be indexed to the calcite phase (JCPDS: 04-0636). Fig. 5(b) shows the result when all Asp solution was initially dumped in crystallization solution. Specific peaks of vaterite are shown on {110}, {112}, {114} phase. All the reflections could be indexed to the vaterite phase (JCPDS: 01-1033). Dropping Asp solution with 2 mL/min leads to the XRD data on Fig. 5(c). Fig. 5(c) shows that calcite and vaterite morphologies exist together. We assumed that dropping Asp significantly affects the formation of vaterite morphology in the initial stage, and the excess amount of Asp results in unstable vaterite morphology. Dropping Asp solution with low velocity (1 mL/min) less influences $CaCO_3$ morphology. However, calcite and vaterite crystals formed together when we added Asp with 2 mL/min.

Composition of calcite and vaterite morphology is identified in detail by XRD spectrometer. Fig. 6 shows the history of $CaCO_3$ crystallization, carried out by using 0.1 M $CaCl_2$ and 0.1 M Na_2CO_3 and dropping Asp solution with 3.4 mL/min. Calcite peak is only identified at 5 min. Vaterite peak appears at 30 min. Intensity of the vaterite peak attains the highest value at 2 hr. Afterward, the intensity of the vaterite peak slowly decreases as the crystallization reaction pro-

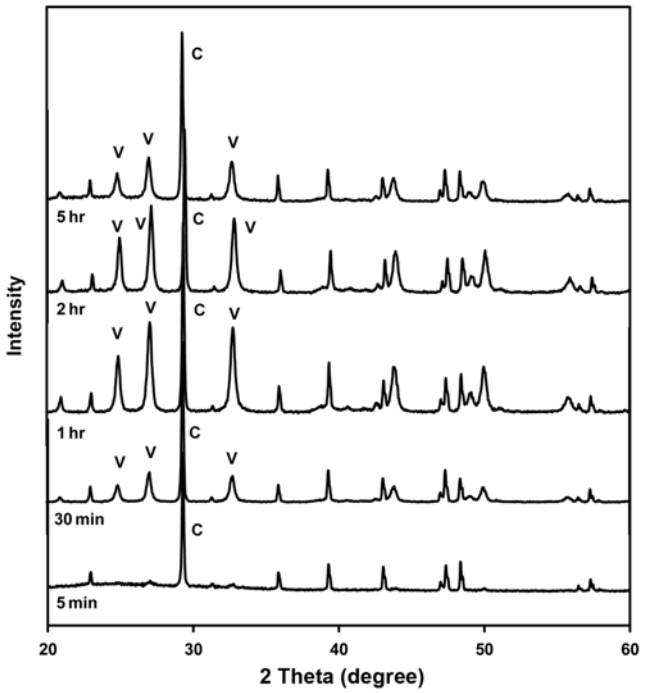

Fig. 6. The change of X-ray diffraction patterns of calcium carbonate crystallized at pH=8.5; dropping speed of Asp=3.4 mL/min.

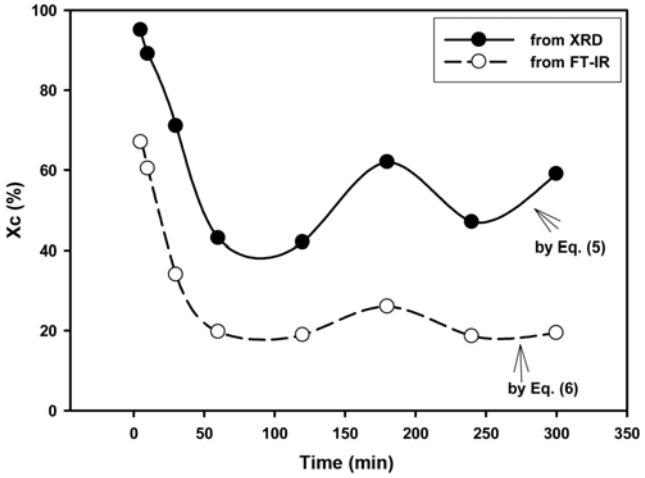

Fig. 7. The change of ratio of calcite to vaterite with reaction time, calculated by using XRD and FT-IR; dropping condition same as Fig. 4.

ceeds. As the effect of dropped Asp solution becomes weak, unstable vaterite transforms to stable calcite. We calculate the ratio of calcite to vaterite with the reaction time by the XRD data.

Fig. 7 illustrates that the ratio of calcite to vaterite (Xc) changes with time under the condition of Na_2CO_3 dropping at 6 mL/min and Asp at 2 mL/min. We utilize XRD data to obtain peak intensities (I) in Eq. (4) and calculate the ratio Xc. Xv means the percentage of vaterite and Xc equals to 100 minus Xc. Eq. (6) explains the calculation method by FT-IR spectral data, in which calcite and vaterite peak areas are obtained by measuring the weight of the peak areas.

$$Xv = \frac{I_{110} + I_{112} + I_{114}}{I_{110} + I_{112} + I_{114} + I_{104}} \times 100 \quad (4)$$

$$Xc = 100 - Xv \quad (5)$$

$$Xc = \frac{\text{Calcite peak area}}{\text{Calcite} + \text{Vaterite peak area}} \quad (6)$$

Xc calculated by Eq. (5) and that by Eq. (6) have similar trend in Fig. 7. Vaterite morphology increases and Xc consequently decreases until 50 min. After that, vaterite transforms to calcite so that Xc increases. Owing to the continuous feeding of Asp, vaterite morphology is generated and its speed higher than the transformation speed to calcite. Hence the rise and fall of Xc could be observed from 100 to 250 min. Xc value by FT-IR spectra fluctuates similarly as the Xc by XRD data, but absolute Xc values by two methods are not matched due to the irregular KBr pellet thickness for FT-IR measurement. Xc value rises and falls once during 60 min in Ref. 29. Compared to the reference, we expect that Xc value could be flexibly controlled by dropping amino acids and/or Na_2CO_3 solution.

SUMMARY

An experimental method was devised to control the polymorphs of calcium carbonate crystals by feeding amino acid solution. Studies were also carried out based on the feeding of Na_2CO_3. Because sodium carbonate produces CO^{3-} in order to form $CaCO_3$ crystals, the feeding of Na_2CO_3 significantly affects $CaCO_3$ crystal morphology.

Since adding amino acids leads to vaterite morphology [22-24], this study also confirmed vaterite morphology. While adjustment of dropping velocity of Gly controlled the ratio of calcite to vaterite [28], this study showed that the ratio of calcite to vaterite was regulated by feeding of Asp and Na_2CO_3.

Polymorphs of $CaCO_3$ crystals were observed by SEM under various dropping conditions of Na_2CO_3 and Asp. Produced calcite crystals at the initial reaction stage were significantly influenced by feeding speed of Asp. Dropping of Na_2CO_3 results in both calcite and vaterite morphologies and shape of crystal is rough due to the effect of Na_2CO_3 feeding.

ACKNOWLEDGEMENT

This research was supported by NRF (Grant No. 20090083674).

REFERENCES

1. A. Devarajan, M. Abdul Khadar and K. Chattopadhyay, *Mater. Sci. Eng. A*, **452**, 395 (2007).
2. Y. Wen, L. Xiang and Y. Jin, *Mater. Lett.*, **57**, 2565 (2003).
3. S. H. Kang, I. Hirasawa, W. S. Kim and C. K. Choi, *J. Colloid Interface Sci.*, **288**, 496 (2005).
4. H. Wei, Q. Shen, Y. Zhao, Y. Zhou, D. Wang and D. Xu, *J. Cryst. Growth*, **279**, 439 (2005).
5. C. Carteret, A. Dandeu, S. Moussaoui, H. Muhr, B. Humbert and E. Plasari, *J. Cryst. Growth*, **9**(2), 807 (2009).
6. W. S. Kim, I. Hirasawa and W. S. Kim, *Ind. Eng. Chem. Res.*, **43**, 2650 (2004).
7. H. Wei, H. Wang, Y. Gao, Y. Zhao, D. Xu and D. Wang, *J. Cryst.*

Growth, **303**, 537 (2007).
8. J. Kawano, N. Shimobayashi, M. Kitamura, K. Shinoda and N. Aikawa, *J. Cryst. Growth*, **237**, 419 (2002).
9. L. Yang, X. Zhang, Z. Liao, Y. Guo, Z. Hu and Y. Cao, *J. Inorg. Biochem.*, **97**, 377 (2003).
10. Y. S. Han, G. Hadiko, M. Fuji and M. Takahashi, *J. Cryst. Growth*, **289**, 269 (2006).
11. H. K. Han, B. M. Kim and J. A. Kim, *Korean Chem. Eng. Res.*, **46**(6), 1056 (2008).
12. W. Hou and Q. Feng, *J. Cryst. Growth*, **282**, 214 (2005).
13. C. G. Kontoyannis, *J. Pharmaceut. Biomed. Anal.*, **13**(1), 73 (1995).
14. C. Shivkumara, P. Singh, A. Gupta and M. S. Hegde, *Mater. Res. Bull.*, **41**, 1455 (2006).
15. F. Manoli, J. Kanakis, P. Malkaj and E. Dalas, *J. Cryst. Growth*, **236**, 363 (2002).
16. W. Hou and Q. Feng, *Mater. Sci. Eng. C*, **26**, 644 (2006).
17. P. Malkaj and E. Dalas, *Cryst. Growth Des.*, **4**(4), 721 (2004).
18. P. S. Lukeman, M. L. Stevenson and N. C. Seeman, *Cryst. Growth Des.*, **8**(4), 1200 (2008).
19. L. Addadi and S. Weiner, *NATURE*, **411**, 753 (2001).
20. T. Takeuchi, I. Sarashina, M. Iijima and K. Endo, *FEBS Lett.*, **582**, 591 (2008).
21. Y. Jiao, Q. Feng and X. Li, *Mater. Sci. Eng. C*, **26**, 648 (2006).
22. F. Manoli, J. Kanakis, P. Malkaj and E. Dalas, *J. Cryst. Growth*, **236**, 363 (2002).
23. F. Manoli and E. Dalas, *J. Cryst. Growth*, **222**, 293 (2001).
24. A. J. Xie, Y. H. Shen, C. Y. Zhang, Z. W. Yuan, X. M. Zhu and Y. M. Yang, *J. Cryst. Growth*, **285**, 436 (2005).
25. J. Xiao, Y. Zhu, Y. Liu, H. Liu, Y. Zeng, F. Xu and L. Wang, *Cryst. Growth Des.*, **8**(8), 2887 (2008).
26. G. E. Henderson, B. J. Murray and K. M. McGrath, *J. Cryst. Growth*, **310**, 4190 (2008).
27. H. Tong, W. Ma, L. Wang, P. Wan, J. Hu and L. Cao, *Biomaterials*, **25**, 3923 (2004).
28. H. Wentao and F. Qingling, *Mater. Sci. Eng. C*, **26**, 644 (2006).
29. J. H. Kim, J. M. Kim, W. S. Kim and I. H. Kim, *Korean Chem. Eng. Res.*, **47**(2), 213 (2009).